

TECNOLOGIA/TECHNOLOGY

BLUFF-BODIES VORTEX SHEDDING SUPPRESSION BY DIRECT NUMERICAL SIMULATION

P. A. R. Ribeiro

Instituto de pesquisas Hidráulicas - UFRGS
 Av. Bento Gonçalves, 9500, 91501-970
 Porto Alegre, RS, Brazil
 parribeiro@yahoo.com

E. B. C. Schettini

Instituto de pesquisas Hidráulicas - UFRGS
 Av. Bento Gonçalves, 9500, 91501-970
 Porto Alegre, RS, Brazil
 bcamano@iph.ufrgs.br

J. H. Silvestrini

Departamento de Engenharia Mecânica e
 Mecatrônica - PUC-RS
 Av Ipiranga, 6681, 90619-900
 Porto Alegre, RS, Brazil
 jorgehs@em.pucrs.br

ABSTRACT

Vortex shedding is responsible for harmful vibrations on immersed structures and for increasing their drag coefficients. Thus vortex shedding suppression is highly interesting in order of decrease maintenance costs of standing structures and fuel costs on moving ones. Vortex shedding suppression is here achieved with the use of splitter plates by means of numerical simulations at a low Reynolds range, Re 100 and 160. For this purpose it has been used a high order finite difference method in association with a virtual boundary method, responsible for the obstacle's representation. The use of this novel numerical method showed a great concordance with experimental results by means of low computational costs.

Keywords: vortex shedding, turbulence, numerical simulation, virtual boundary method.

INTRODUCTION

Vortex shedding from circular cylinders have always been a subject of interest, both for experimentalists and for numerical researchers, thanks to its geometrical simplicity in addition to its practical importance in engineering. Nevertheless the flow at low Reynolds numbers has recently achieved great attention due to the advances on the understanding of three-dimensional developments on circular cylinder wakes, after studies carried out by Williamson (1989) on the discontinuity on the Strouhal-Reynolds curve around $Re = 70$, and Williamson (1996) on the recognition of vortex shedding Mode-A and Mode-B for wake transient régimes.

Since then, the spotlights have focus on the understanding of flow instability phenomena and on its control of vortex shedding. A fine summary of vortex shedding control techniques is carried out by Schumm et al. (1994), the authors present two families of vortex shedding control techniques: the open-loop control techniques, i.e. those who introduce physical changes on the obstacle, such as the use of geometrical disturbances, splitter plates, wall rotation among others; and the close-loop control techniques that consist of changing the flow characteristics just like base bleed, base suction, wake heating, control wire, feed-back control, etc.

Among this techniques the use of splitter plates is surely one of the first approaches studied, Roshko (1954) presents experiments using splitter plates where he shows that vortex shedding can be completely suppressed at $Re = 1,45 \times 10^4$ for a plate length l equal to $5D$, where D is

the cylinder's diameter. Bearman (1965) showed that the vortex shedding suppression for square cylinders with splitter plates at Reynolds numbers between $1,4 \times 10^5$ and $2,56 \times 10^6$ occurs, for all cases studied, for $l/D = 3$.

There are few numerical simulations concerning the transient wake régime, $100 < Re < 300$, for example one can quote Know and Choi (1996) who studied vortex shedding suppression with splitter plates for Reynolds numbers between $80 < Re < 160$, avoiding this way the three-dimensionality that occurs for Reynolds numbers higher than 160. In this paper numerical simulations were performed at $Re = 100$ and $Re = 160$ finding a great agreement with the previous authors results. There are presented as well some results at $Re = 300$ where one finds some puzzling features on the interaction between the plate's boundary layer and the wake structures.

NUMERICAL METHODS

Uncompressible flows were simulated using the governing equations

$$\vec{\nabla} \cdot \vec{u} = 0 \quad (1)$$

$$\frac{\partial \vec{u}}{\partial t} + \vec{u} \cdot \vec{\nabla} \vec{u} = -\frac{1}{\rho} \vec{\nabla} p + \nu \nabla^2 \vec{u} + \vec{f} \quad (2)$$

On these equations one has ν as kinematic viscosity, $p(\vec{x}, t)$ the pressure field, $\vec{u}(\vec{x}, t)$ the velocity field and

$\vec{f}(\vec{x}, t)$ the external forcing field, used to represent the virtual boundary.

This external forcing field, introduced by Goldstein et al. (1993), can be described as a harmonic oscillator like

$$\vec{f}(x_s, t) = \alpha \int \vec{u}(x_s, t) dt + \beta \vec{u}(x_s, t) \quad (3)$$

The time integration has been done using a low-storage third-order Runge-Kutta scheme introduced by Williamson (1980), and spatial derivatives were calculated using a sixth-order compact finite difference scheme presented by Lele (1992) over a cartesian uniform grid. Boundary conditions were set to be semi-periodic on y and non-periodic on x , as presented at Figure 1. More details about the numerical code and the immersed boundary methods used can be found in Silvestrini and Lamballais (2002) and Lamballais and Silvestrini (2002).

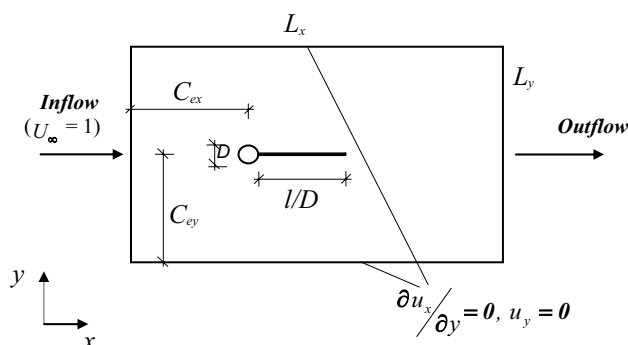


Figure 1. Flow configuration.

COMPUTATIONAL DOMAIN

Computational domain defined by $L_x = 19D$, $C_x = 6D$, $C_y = 6D$ with mesh grid size $D = 24\Delta$ for the two dimensional simulations and $D = 18\Delta$ for the three dimensional, have minimized the confinement effects, the flow oscillation in front of the obstacle and computational costs. More details can be seen at Ribeiro (2002).

TWO DIMENSIONAL FLOW AROUND CYLINDERS WITH SPLITTER PLATES

It is known that vortex shedding may be suppressed by the introduction of splitter plates on the wake of bluff-bodies. Roshko (1993), per example, affirms that depending on cylinder cross-section shape, a plate length of 7 to 10 diameters is sufficiently long for the near wake to be independent of that length. Usually this phenomena is used as a model to analyze the role of the separated shear layers and drag, like in the works of Arie and Rouse (1956), Roshko (1954) and Roshko (1993).

Perhaps, one of the first attempt to understand the role of three-dimensionality on the shedding of bluff-bodies with attached plates is introduced by Bearman (1965), who described régimes on the variation of Strouhal number on different plate lengths for a square cylinders at Reynolds numbers between $1,4 \times 10^5$ and $2,56 \times 10^6$, in all cases he found vortex shedding suppression for $l/D = 3$.

On a numerical attempt of finding this same phenomena, Know and Choi (1996) studied vortex shedding suppression for the two-dimensional wake

régime, $80 \leq Re \leq 160$, and these authors found great agreement with Bearman's results.

The present simulations at $Re = 100$ showed great agreement with those obtained by Know and Choi (1996), vortex shedding has been suppressed for a plate length equal to $l/D = 3$, and for l/D equal to 1 and 2 values differ 3,6% and 7,5% respectively, as can be seen at Figure 2.

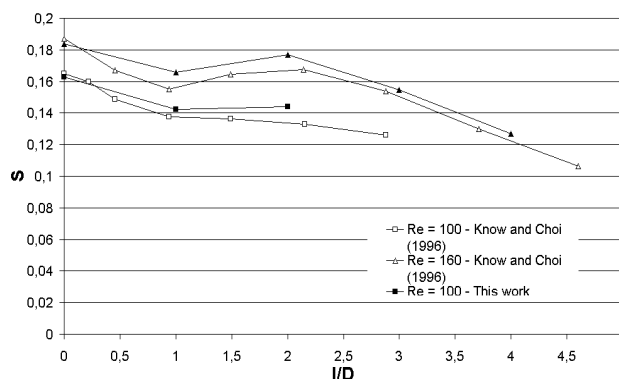


Figure 2. Strouhal number vs. plate length behind circular cylinder at $Re = 100$ and $Re = 160$.

Those differences may be interpreted as influence of an extensively greater domain by the first authors, $-50D < x < 20D$ and $-50D < y < 50D$, and the use of a finer mesh near the cylinder. Nevertheless it is very important to emphasize that these simulations that solve the Navier Stokes over a curvilinear mesh consumes enormous time and computational resources compared by those performed in this work over a uniform cartesian mesh, which also achieve great results, being possible better used based on a cost effectivity criteria.

In Figure 3 one can see qualitatively the wake's behavior due the plate's presence at $Re = 100$. The clearly represented vortex street of Figure 3a suffers a strong reduction on its shedding frequency when there is the plate's introduction, until the flow reattaches to the plate and vortex shedding is simply suppressed, Figure 3b.

Figure 4 shows vortex shedding suppression at $Re = 160$, being suppressed for l/D equal to 5, which agree with numerical experiments presented by Know and Choi (1996) that define the critical plate length as $4,6D$.



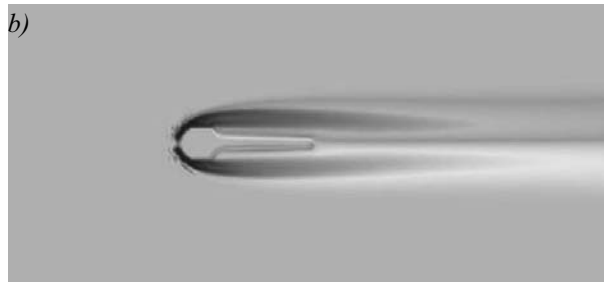


Figure 3. Vorticity field for $Re = 100$ at time $t \cdot U_\infty / D = 347$; a) $l/D = 2$, b) $l/D = 3$.

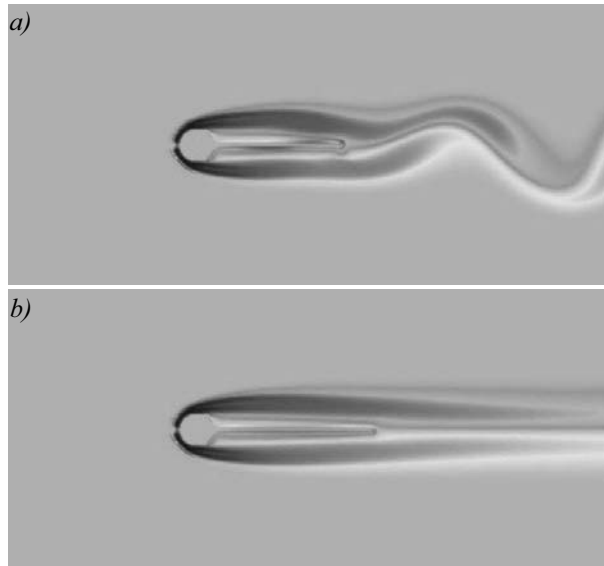


Figure 4. Vorticity field for $Re = 160$ at time $t \cdot U_\infty / D = 248$; a) $l/D = 4$, b) $l/D = 5$.

It is truth that for Reynolds numbers higher than 170 that the three-dimensionality has a major role, which could suggest that two-dimensional simulations are not able to represent its features. But in terms of shedding frequency this is not the truth at all once one gets to the Reynolds numbers higher than 250. In these cases the Strouhal numbers resulting are slightly affected by the three-dimensionality, in such a way that two-dimensional simulations achieve similar shedding frequencies, as one can see comparing the experimental data against the 2D simulations on Figure 5. This way it was found worth to analyze two-dimensionally this flow patterns, always concerning that one might be very careful to jump into conclusions after these two-dimensional simulations results.

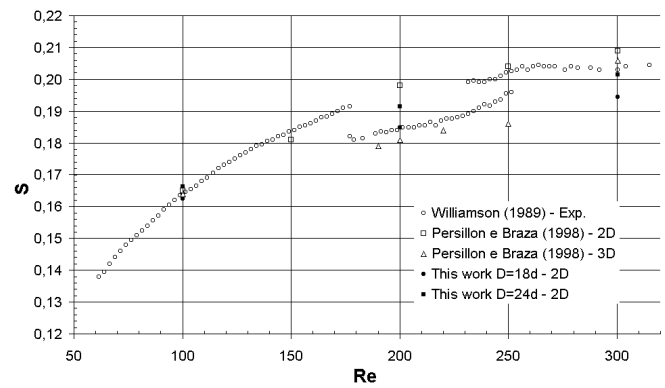


Figure 5. Strouhal number vs. Reynolds number; experimental and numerical results.

Simulations at $Re = 300$ for cylinders with attached splitter plates were performed for plate lengths, l/D , ranging from 0 to 10. The results obtained by the present simulations are plotted together with other results showing an interesting phenomena on Strouhal Number as one increases the plate length Figure 6.

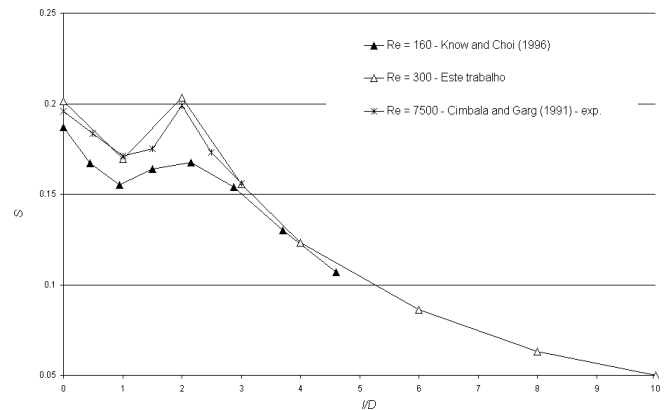


Figure 6. Strouhal number vs. plate length behind circular cylinder for different Re .

There is a notable increasing on the Strouhal number for the plate lengths $1 < l/D < 2$. Bearman (1965) suggests that this phenomena is associated to a critical length where the plate induces the vortices to break down from the shear layers upstream to the end of the plate, developing not fully formed vortices. The present results for $Re = 300$ showed to be unable to correctly represent this phenomena due to the small number of simulations performed until this moment, but partial results show a increase of 1% on the Strouhal number for $l/D = 2$, and an great decrease for further lengths, as shown in Figure 7.

There is a notable increasing on the Strouhal number for the plate lengths $1 < l/D < 2$. Bearman (1965) suggests that this phenomena is associated to a critical length where the plate induces the vortices to break down from the shear layers upstream to the end of the plate, developing not fully formed vortices.

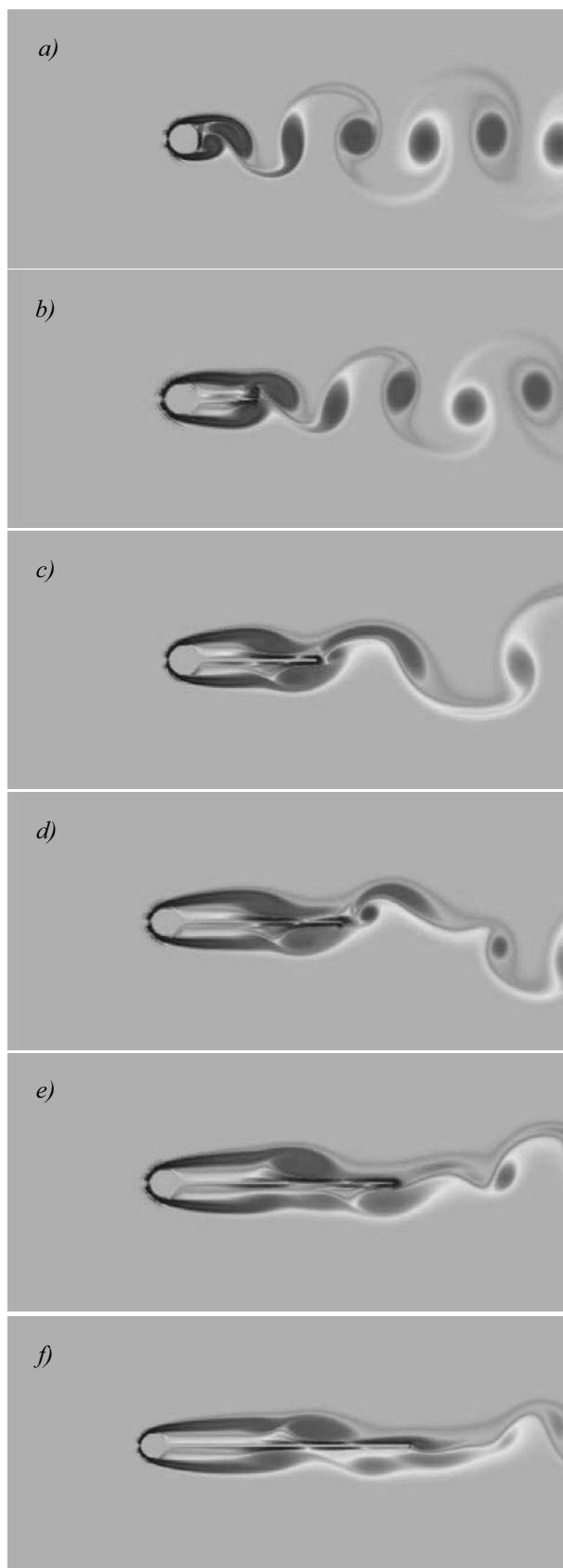


Figure 7. Vorticity field for $Re = 300$ at time $t^*U_\infty/D = 248$; a) no plate, b) $l/D = 2$, c) $l/D = 4$, d) $l/D = 6$, e) $l/D = 8$ e f) $l/D = 10$.

The present results for $Re = 300$ showed to be unable to correctly represent this phenomena due to the small number of simulations performed until this moment, but

partial results show a increase of 1% on the Strouhal number for $l/D = 2$, and an extraordinary decrease for further lengths.

In the $Re = 160$ simulations appears an interesting vortex at the edge of the plate. This structure had already been recognized by Know and Choi (1996) but no further study about it's formation and influence on the flow have been found. In this work this eddy formation could be found also at higher Reynolds numbers, where it looks stronger and better defined.

Due to the presence of the plate, the shear layer that starts on the surface of the cylinder generates vorticity of opposite signal over the plate, as one can see following vortices B and B' in Figure 8a.

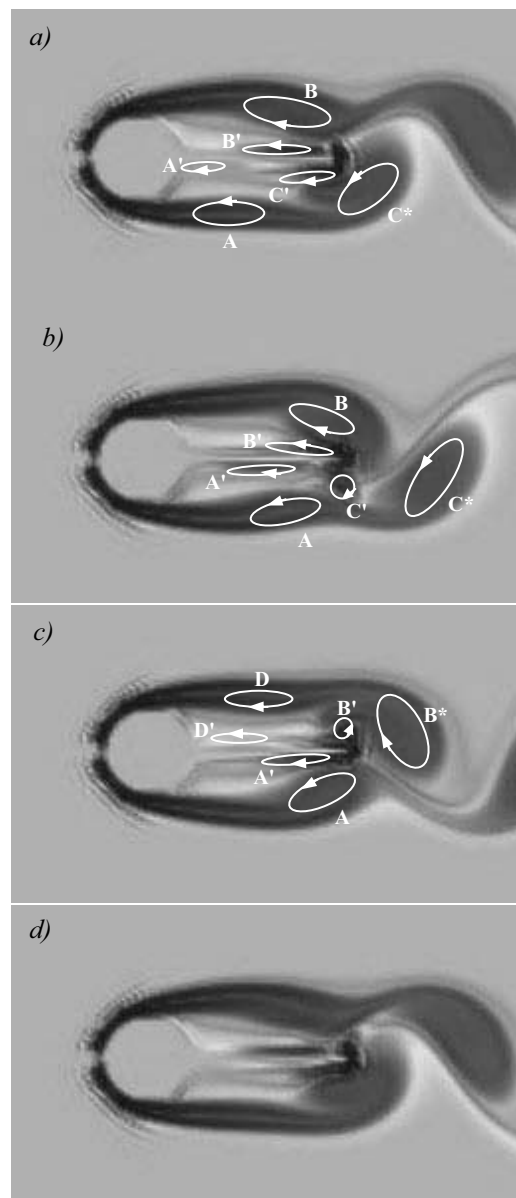


Figure 8. Vorticity field for $Re = 300$ and $l/D = 2$. $\Delta t^*U_\infty/D$ between each image equal to 1,49.

Vortex B' moves together with vortex B along the plate, while at this same moment vortex C' is ahead of vortex B' and gets trapped at the end of the plate by vortex C*. At Figure 8b vortex B' gets trapped on the plate's edge while vortex C' is paring with vortex B.

At Figure 8c vortex B* is the result of the pairing between vortices C' and B, and it traps the growing vortex B' that can be seen pairing with vortex A at Figure 8d, where there is again nearly the same vorticity field as in the first image.

In order to study how this vortex frequency influence the wake, the velocity signals and their respective frequency spectrums have been analyzed at several positions over the domain, as shown in Figure 9.

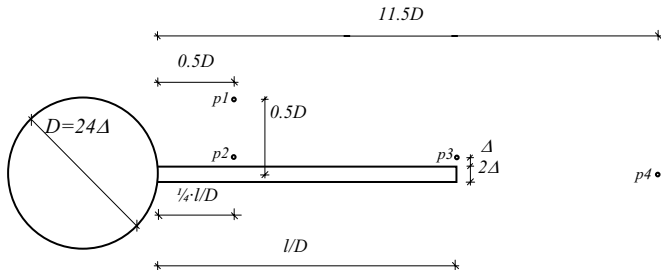


Figure 9. Location of probes near the obstacle.

The probe $p1$ has been placed to achieve the breaking shear layer's signal, while probes $p2$ and $p3$ are placed to get the velocity signals near the plate's surface respectively before and at the plate's edge, finally probe $p4$ has been placed to get the frequency spectrum at the wake.

As one can see in Figure 10 the power spectrum density on the wake for $Re = 300$ ($x/D = 1$, $y/D = 0$), on a situation with no plate has well defined peaks which are stronger on the odd multiples of the main frequency.

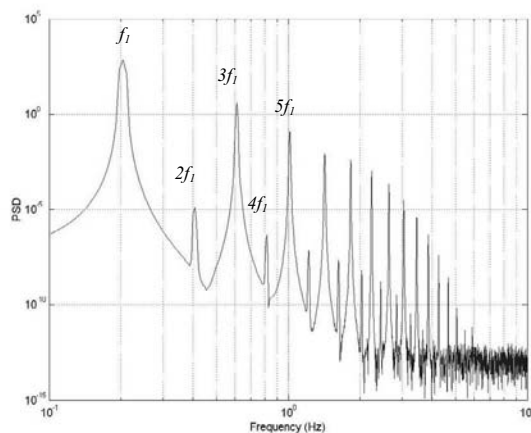


Figure 10. Power Spectrum Density at $Re = 300$ for a circular cylinder with no splitter plate, $x/D = 1$, $y/D = 0$.

This spectrum behavior changes slightly with the plate's presence at the $p1$ location as seen at Figure 11a. Here the signal is expected to be barely affected by the presence of the plate. In fact one can take note of the absence of higher frequencies and that there is not much difference between odd and even multiples.

The same behavior is verified at $p2$ (but the signal has less energy), Figure 11b, suggesting that at these locations there is a direct interaction between the shear layer and the boundary-layer over the plate.

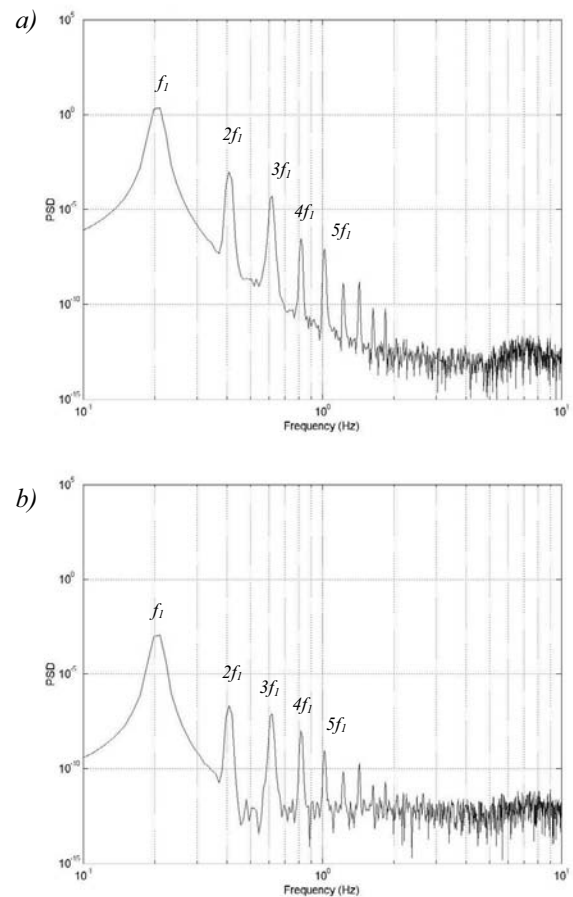


Figure 11. Power Spectrum Density for $Re = 300$ and $l/D = 2$. a) $p1$ and b) $p2$.

One can see at $p3$ frequency spectrum, Figure 12a, the clear presence of higher frequencies, not strong on the previous signals, suggesting that this new frequencies are associated with the growth of the eddy at the plate's edge.

At $p4$ location one finds a frequency spectrum very similar to the one of the flow without plate, Figure 12b. But in comparison with $p1$, $p2$ and $p3$ spectra one can clearly notice less energy on the odd multiple of the main frequency.

CONCLUSIONS AND DISCUSSIONS

The virtual boundary method used together with a uniform cartesian mesh, in comparison to the solution of the Navier-Stokes equations over a body-fitted mesh with curvilinear coordinates, permits the use of a small computational demand obtaining satisfactory results.

The use of splitter plates to control bluff-bodies' vortex shedding shows to be of great efficiency. As it has been shown, attached plates perform great changes on the shedding frequency depending on the length.

At first, the end plate vortex seemed to have a major role on the shedding frequency, but further studies showed that it has no influence on the major frequency, and its shedding is governed by the Kármán vortex trail and by the recirculation region behind the obstacle.

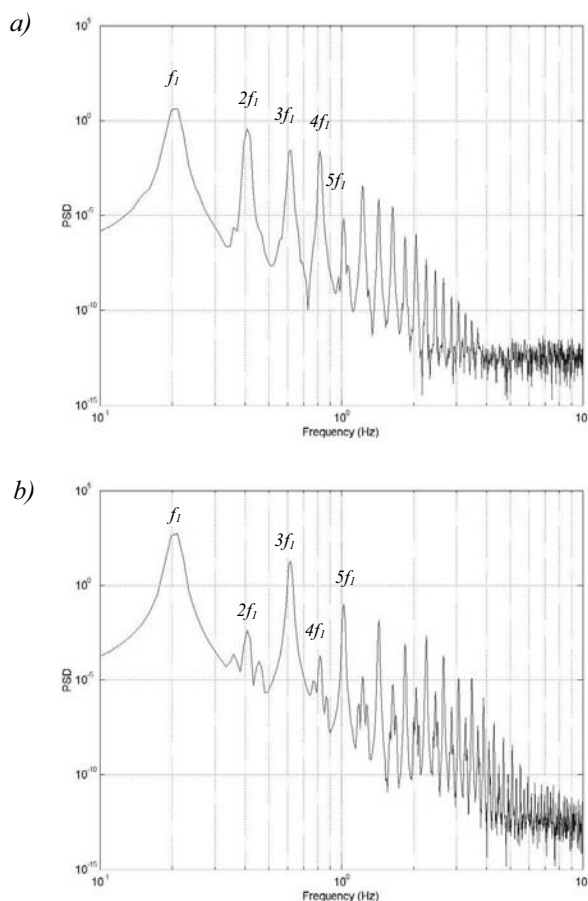


Figure 12. Power Spectrum Density for $Re = 300$ and $l/D = 2$. a) $p3$ and b) $p4$.

ACKNOWLEDGEMENT

The authors wish to thank the support provided by the Pontifícia Universidade Católica do Rio Grande do Sul, by means of its computational resources and staff, the Instituto de Pesquisas Hidráulicas of the Universidade Federal do Rio Grande do Sul and the Conselho Nacional de Desenvolvimento Científico e Tecnológico – CNPq for sponsoring this project.

REFERENCES

- Arie, M. and Rouse, H., 1956, "Experiments on two-dimensional flow over a normal wall", *Journal of Fluid Mechanics*, Vol. 1, Part 2.
- Bearman, P. W., 1965, "Investigation of the flow behind a two-dimensional model with blunt trailing edge and fitted with splitter plates", *Journal Fluid Mechanics*, Vol. 21, part 2, p. 241-255.
- Berger, E. and Wille, R., 1972, "Periodic flow phenomena", *Ann. Rev. Fluid. Mech.*, Vol. 4, p. 313-340.
- Cimbala, J. M. and Garg, S., 1991, "Flow in the wake of a freely rotatable cylinder with splitter plate", *AIAA Journal*, Vol. 29, p. 1001-1006.
- Goldstein, D., Handler, R. and Sirovich, L., 1993, "Modeling a no-slip flow boundary with an external force field", *Journal of Computational Physics*, Vol. 105, p. 345-366.

Know, K. and Choi, H., 1996, "Control of laminar vortex shedding behind a circular cylinder using splitter plates", *Physics of Fluids*, Vol. 8, No. 2, p. 479-486.

Lamballais, E. and Silvestrini, J., 2002, "Direct numerical simulation of interactions between and mixing layer and a wake around a cylinder", (in press) *J. of Turbulence*.

Lele, S. K., 1992, "Compact finite difference schemes with spectral-like resolution", *Journal of Computational Physics*, Vol. 103, p.16-42.

Pérsillon, H. and Braza, M., 1998, "Physical analysis of the transition to turbulence in the wake of a circular cylinder by three-dimensional Navier-Stokes simulation", *Journal of Fluid Mechanics*, Vol. 365, p. 23-88.

Ribeiro, P. A. R., 2002, "Desprendimento de vórtices e controle em esteira de cilindros por simulação numérica direta". Dissertação de Mestrado – IPH, UFRGS.

Roshko, A., 1954, "On the drag and the shedding frequency of two-dimensional bluff bodies", *NACA TN 3169*, 29 p.

Roshko, A., 1993, "Perspectives on bluff body aerodynamics", *Journal of Wind Engineering and Industrial Aerodynamics*, Vol. 49, p. 79-100.

Saiki, E. M. and Biringen, S. 1996, "Numerical simulation of a cylinder in uniform flow: application of a virtual boundary method", *Journal of Computational Physics*, Vol. 123, p.450-465.

Schumm, M., Berger, E. and Monkewitz, P. A., 1994, "Self-excited oscillations in the wake of two-dimensional bluff bodies and their control", *Journal of Fluid Mechanics*, Vol. 271, p.17-53.